Environment and Planning B: Planning and Design 2008, volume 35, pages 399 – 412

doi:10.1068/b33046

A shape-based buffering method

Lan Mu
Department of Geography, University of Georgia, Athens, GA 30602, USA;
e-mail: mu@uga.edu
Received 5 May 2006; in revised form 7 January 2007; published online 22 February 2008

Abstract. Distance constraint is a major concern in many spatial analyses. Buffering is one of the proximity techniques in GIS most commonly used to address this constraint. I introduce shape-based point buffering, an anisotropic and variable-distance buffer generation method conformal to the original polygons. In contrast with isotropic fixed-distance buffering, shape-based buffering is defined using a relative distance (percentage) instead of a real unit (for example, meters), and it allows all buffered boundaries to be formed at the same time. The construction and implementation of the buffering method are described below. Three emergency-response scenarios are designed to demonstrate potential applications of this buffering method, including a shape-based fixed-percentage buffer calculation and space distribution, a shape-based variable-percentage buffer region, and a reverse calculation of the task schedule from a probability surface constructed from shape-based buffers. Limitations of the method are discussed. The method has potential applications in emergency preparedness and planning to better address fairness issues when a geographic area must be zoned arbitrarily.

Introduction—buffer analysis in GIS

Buffering is one of the most commonly used proximity techniques in GIS, because distance constraint is a major concern in many types of spatial-analysis applications, such as emergency preparedness, business development, and school districting. A buffer is a zone with a specified distance surrounding a spatial feature, and the process of creating a buffer is called buffering. Among the many buffering methods, distance-based buffering is the simplest. This paper introduces an alternative, shape-based buffering, which is a buffer generation method conformal to polygon constraint.

Types of buffer analysis and applications

Buffers can be categorized as simple, compound, or nested (Bolstad, 2005). Simple buffers can be classified as fixed-distance versus variable-distance, and as isotropic versus anisotropic. A fixed-distance buffer applies one or more fixed distance parameters to all features, and a variable-distance buffer applies varied distance parameters to different features. An isotropic buffer applies the same distance in all directions around any individual feature, while an anisotropic buffer dilates by different distances in different directions. Fixed-distance buffers and variable-distance buffers may be isotropic or anisotropic. Many existing buffer operations are isotropic. Figure 1 differentiates the four categories of buffer. GIS applications can be found for each of the categories in figure 1. We review some examples.

Isotropic fixed-distance buffering is the simplest and most straightforward type of buffering technique. It has been used, for example, to depict uniform half-mile buffers which serve as the trading areas of all supermarkets in Leeds (UK) city postal sectors. The simple 'buffer and overlay' method is then compared with a more sophisticated spatial interaction model to plan for retail-store locations (Benoit and Clarke, 1997). In Sydney, Australia, it was used to define areas subject to disaster risk, first by delineating a 100 m buffer zone on both sides of residential streets to define the residential

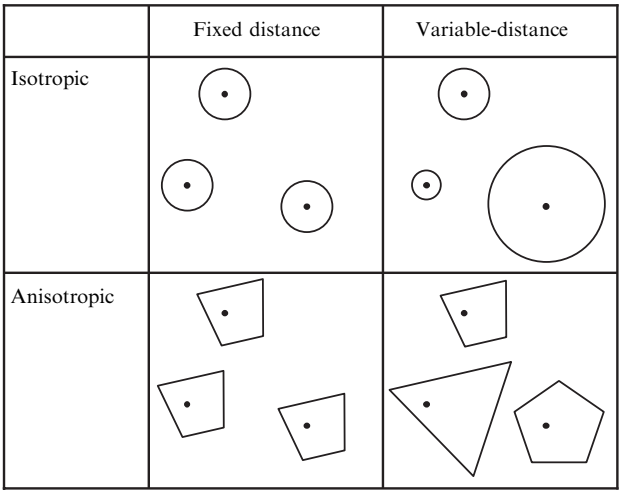

Figure 1. Types of simple point buffers.

land-use area, then using this output as the input for a catastrophe loss-estimation model (Chen et al, 2004). Another example of its application is the identification of environmental features which influence the distribution of paramphistomosis (a rumen fluke) in sheep in the southern Italian Apennines. Here, 3 km buffer zones centered on each of the 197 farms in the subject region are used as templates to collect environmental variables such as vegetation index, land cover, elevation, slope, aspect, and total length of waterways, combined with field data collected by veterinarians. This buffer-zone data-compilation method has proved to be a simple but effective way to test the statistical significance of environmental variables with respect to a farm's infection status (Cringoli, et al, 2004). To predict average concentrations of traffic-related air pollutants, fixed-distance buffer zones ranging from 100 m to 10 km are sampled to aggregate traffic flow with measurements of pollutants. A buffer distance of 1 km is chosen for explaining small-scale (local) variations, and a buffer distance of 3 km or more is used for large-scale (urban and surrounding rural area) predictions (Hochadel et al, 2006). Other examples of isotropic fixed-distance buffer applications include studies of the impact zones of amphibian species in Stockholm (Löfvenhaft et al, 2004), the measurement of loon mercury levels (Kramar et al, 2005), riparian zones for non-point-source pollution (Narumalani et al, 1997), influencing areas of environmental epidemiological processes (Vine et al, 1998), the unequal relationship between the built environment and health disparities in physical activity and obesity (Gordon-Larsen et al, 2006), accuracy assessment of georeferencing errors for lateral channel movements (Hughes et al, 2006), subgroup definition of small mammals from point sampling (Pocock et al, 2003), the involvement of herbivory and bush products in the spatial distribution of savanna types (Ringrose et al, 1996), and water quality monitoring in urban areas (Yin et al, 2005).

Isotropic variable-distance buffering assumes that the buffer will be developed equally in all specified directions; however, the buffer distance is not uniform for every feature, but is assigned, based on the value of a variable. The variable could be, for example, the capacity of a hospital or the spread speed of a chemical release. To study the uncertainty in potential-connectivity analysis of red squirrels in a fragmented landscape, a variable-distance buffer based on the friction values of a fuzzy set was compared with a traditional fixed-distance 1 km Boolean buffer (De Genst et al, 2001). To assess government health service use in Kenya by children with fevers, a variable-distance

buffer based on Thiessen polygon areas was created to study catchment areas and reduce overlaps (Gething et al, 2004). To explore the spatial patterns of asthma and air pollution in Bronx, New York, in the context of environmental justice, a combined four-layer buffer (toxics-release inventory, stationary-point-source pollution, major truck routes, and limited access highway) was created on the basis of different geometric shapes and distances (Maantay, 2007). Other applications of this type include evaluating the impact of airborne toxic releases on populations with special needs (Chakraborty and Armstrong, 2001), and highway noise mitigation for environmental justice (Chakraborty et al, 1999).

Anisotropic fixed-distance buffering is a variant of isotropic fixed-distance buffering. These buffers have direction sensitivity; that is, for each feature, the buffer has a different distance in a different direction. However, buffer distance for each direction is a fixed value for all features. A good example of anisotropic fixed-distance buffering is a fire-spreading process based on wind speed when the landscape and fuel (vegetation type) are uniform in the simulation space. Wind speed in each direction determines buffer distance at any point in time. Applications of such simulations include wildlife evacuation-trigger buffering (Cova et al, 2005) and urban fire-hazard modeling for emergency preparedness (Radke, 1995; Radke et al, 2000).

Anisotropic variable-distance buffering aims to handle more realistic situations. Many buffers in the real world are not simple geometric shapes, but rather are derived from environmental interactions or expert input based on knowledge of the study area's topography, soil, land use, property ownership, and other factors. For example, GIS-based riparian buffer analyses were conducted on North Carolina watersheds to delineate variable-distance buffers through the injection into the model of environmental or expert information such as soil, slope, vegetation, and scenic quality (Xiang, 1993; 1996; 1998; Xiang and Stratton, 1996). Buffering was applied to the delineation of biosphere reserves in New Jersey Pinelands based on the theory of island biogeography, according to which, ecosystem management can be operated by identifying core areas of high ecological value, and surrounding them with protective buffers (Walker and Solecki, 1999).

In many urban planning applications, the simple GIS applications of the buffer (isotropic and fixed-distance) and overlay approach can only initiate the modeling of spatial competition among factors. More sophisticated measurements, such as potential values, potential coefficients, fuzzy choice value, and land use, are required to improve such access modeling. The final form of the outcomes is often anisotropic with varied distances (De Jong and Ritsema van Eck, 1996). To assess the effectiveness of a protected area in southeast Mexico, for example, the standard buffer area (fixed-distance) was compared with a similar variable-distance buffer area which included environmental variables. The results show the standard fixed-distance method overestimates the protective power of the resulting buffer area (Mas, 2005).

The shape-based buffering introduced in this paper differs from the buffering methods described above, and is characterized as anisotropic and variable-distance. I outline below the necessity of, and motivation for, the development of such a buffering method.

Opportunities and constraints in buffer analysis

The various buffering techniques used in spatial-data analysis each have advantages and drawbacks. For instance, in a water-quality analysis, water-chemistry variables are found to be better correlated with buffer zones than with entire catchment areas (Sliva and Williams, 2001). In GIS applications, the buffer technique has proven more effective than length and area methods in the context of sketch-map analysis, where the

conformal (shape-preserved) requirement is critical (Okamoto et al, 2004). To overcome the limitations of fixed-distance buffers and simple geometrically overlaid buffers, a mutually exclusive and linked on–off network method is created to improve buffer analysis of complex network features (Upchurch et al, 2004). A buffer definition based on an accessibility surface, a minimal cumulative resistant (MCR) surface, is constructed by connecting equal MCR contour lines. Such an approach can help to identify security patterns in landscape ecological planning (Yu, 1996). Alternative methods of buffer formation have been proposed in order to overcome the shortcomings of proximity buffers (equivalent to the distance-based buffers discussed in this paper) in many GIScience research papers (Pereira, 2004).

In many situations buffering is constrained by boundaries, such as physical and social regions. Voronoi diagrams (or Thiessen polygons) are often used in location-allocation analysis to assign service or influence areas for point data. The buffer and overlay approach is often coupled with the Voronoi method to analyze the accessibility of geographical locations. Reliance on this approach, however, has limitations and drawbacks, such as overlooking transportation networks and natural or manmade barriers, assuming equal weighting within a Voronoi diagram or an assigned buffer zone, ignoring competition with established services, and disregarding the capacity level of services (De Jong and Ritsema van Eck, 1996). Four types of error indicators in vector-based buffer analysis have been identified and statistically examined—the error of commission, the error of omission, the discrepant area, and the normalized discrepant area (Shi et al, 2003).

Buffering and the Voronoi diagram are fundamentally related. Assuming a set of points follows an isotropic fixed-distance buffering process, the buffers can meet eventually and delineate the resulting space as Voronoi diagrams of the point set, as shown in figure 2(a). The assumption in such a process is that any location will be assigned to the closest buffer zone, which is equivalent to the concept behind the ordinary Voronoi diagram. The Voronoi diagram provides the most intuitive approach for assigning influence regions for points, especially when the underlying process and boundary information are not available. If we accept the Voronoi diagram as the final space assignment of a set of points, and given that the isotropic fixed-distance buffer-growing process begins simultaneously from each point, then there exists a conceptual problem of simultaneity. Why are the boundaries of Voronoi polygons not formed at the same time [in figure 2(a), the number of buffer rings is not the same for each polygon or for each direction]? Given the simplicity and limitations of Voronoi diagrams, I propose a shape-based buffering method to address the conceptual question of simultaneity.

A shape-based buffering method

A variation of Voronoi diagrams with V-distances

In the family of Voronoi diagrams, the planar ordinary Voronoi diagram (or Thiessen polygon) has very restrictive requirements for point location, weight rules for assignment or growth, and space [usually two dimensional (2D)]. Relaxing any one requirement will yield generalized Voronoi diagrams. Conventionally, an assignment rule used to generalize a Voronoi diagram is called a V-assignment rule, and the distance between any point in the space and its assigned Voronoi generator point is called the V-distance. Therefore, "we can define a generalized Voronoi diagram with any distance as long as the distance is a V-distance" (Okabe et al, 2000, page 189). To develop a shape-based buffering method, I use the shape of Voronoi polygons as a starting point. Later, we show that the shape can be modified to any convex shape. I consider our method to be a variation of Voronoi diagrams with V-distances, particularly the subtype with convex distance.

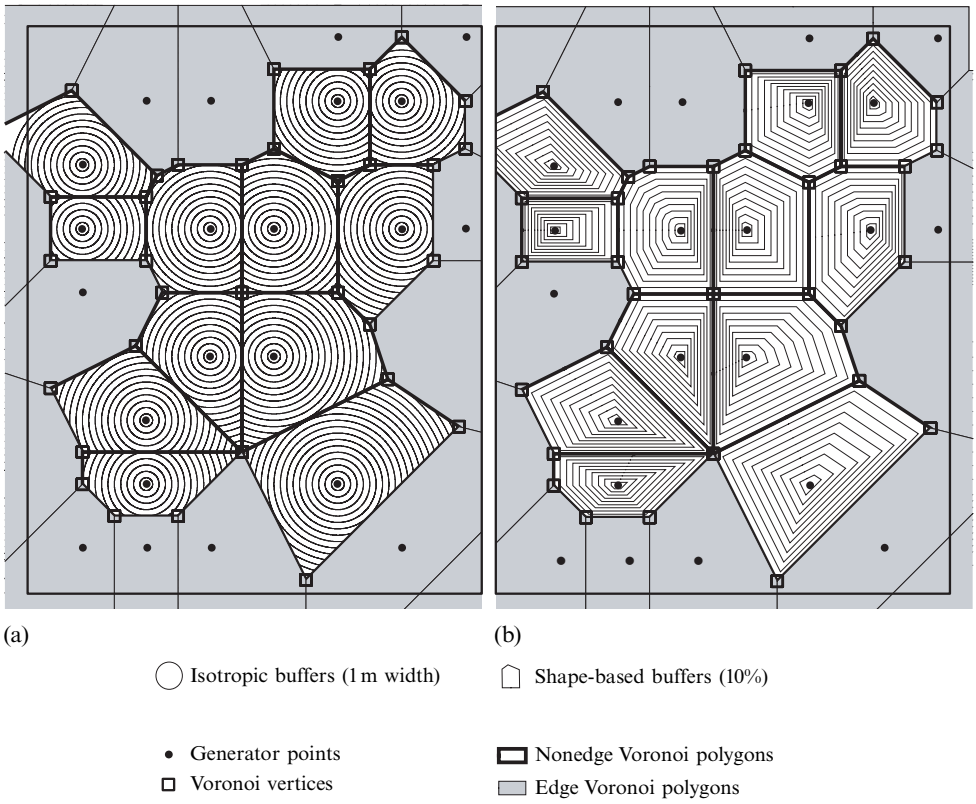

Figure 2. Comparison between Voronoi diagrams for (a) isotropic distance-based buffers and (b) shape-based buffers.

A Voronoi diagram with convex distance is a particular type of the generic V-distance Voronoi diagram. In a 2D space (figure 3), let C be an arbitrary convex figure (for example, a triangle), o the origin of the coordinate system, p a fixed point (for instance, a generator point in a Voronoi diagram), p_i any point in the space, and λ the scaling factor ($\lambda > 0$), which scales C up or down concentrically. The notation C_p implies the reference point of C (say, the interior point of a triangle) is placed at p, and C_o is the standard position of C_p. The scaled up (down) convex figure can be represented as $C_{p,\lambda}$. The convex distance between points p and p_i, $\mathrm{d}_{\mathrm{conv}}(p, p_i)$, is defined as the minimum value of λ to include p_i in $C_{p,\lambda}$. Mathematically, $\mathrm{d}_{\mathrm{conv}}(p, p_i)$ is defined by

$$\mathrm{d}_{\mathrm{conv}}(p, p_i) = \min\{\lambda | p_i \in C_{p,\lambda},\ \lambda > 0\} \ . \tag{1}$$

Expanding the definition of the convex distance between points, other formats of the convex distance can be defined, such as $\mathrm{d}_{\mathrm{conv}}$ from a point to a polygon, and $\mathrm{d}_{\mathrm{conv}}$ from a polygon to a polygon (Okabe et al, 2000).

The uniqueness of the convex distances derives from the transformation of the distance measurement to a ratio of λ. When the convex shape is a circle, the convex distance becomes the Euclidean distance. The choice of other shapes, such as an ellipse or a triangle, broadens the use of Voronoi diagrams with V-distances to applications such as robot motion planning.

The shape-based buffering method is inspired by the Voronoi diagram with convex distance and is developed under the following circumstances—the choice of the

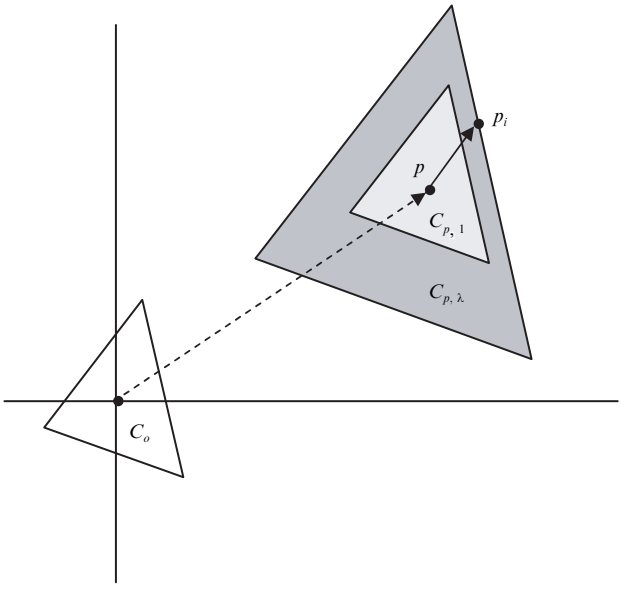

Figure 3. Convex distances specified by a triangle (permission granted: revised from figure 3.7.7 on page 195 of Okabe, 2000).

convex shape varies for each generator point, the shapes exist a priori (for example, predetermined by the ordinary planar Voronoi diagram), and the scaling factor λ is a percentage ranging from zero to one hundred. Details are discussed below.

Construction of shape-based buffers

Figure 2 demonstrates the conceptual idea behind shape-based buffering using Voronoi polygons. There are thirty generator points in the dataset. The boundaries of the Voronoi diagram, the polygons, are shown in solid black lines. The edge polygons (in gray) are masked out to eliminate the uncertainty caused by edge effects. Figure 2(a) shows an isotropic fixed-distance buffering. The width of each ring is 1 m. The buffers have between five and twenty-one rings before reaching the boundary of the Voronoi diagram. Following this buffering process, the boundaries do not form simultaneously. Figure 2(b) shows a design of the shape-based buffers. The buffers do not grow symmetrically. Instead, the Voronoi diagram predetermines the shape of the buffers. The buffers grow unevenly in different directions. In this example, each buffer grows at 10% increments in different directions, that is, $\Delta\lambda = 10\%$. At the tenth step, all buffers reach the Voronoi boundaries. This method is designed to satisfy three assumptions—all points exist from the beginning, any location in the space belongs to a buffer zone closest to one (or more) generator point(s), and all Voronoi boundaries are formed simultaneously. Addressing the earlier discussion of the opportunities and constraints of buffer analysis, the first two assumptions are designed to take advantage of the simplicity of Voronoi diagrams, and the third assumption is crafted to address the problem of simultaneity. Compared with isotropic fixed-distance buffering, shape-based buffering is shape-conformal (eg, Voronoi polygons), anisotropic, and defined using relative distances (percentages) instead of real units (eg, meters).

After the conceptual model is designed, the construction of the shape-based point buffers is mathematically straightforward. In figure 4, let g be a generator point, and v_i ($i = 1, 2, \ldots, n$) any vertex point of the Voronoi polygon V_g of g. V_g has a total of n vertices. Let B_g be a shape-based buffer of point g. Since B_g is conformal to V_g it also has

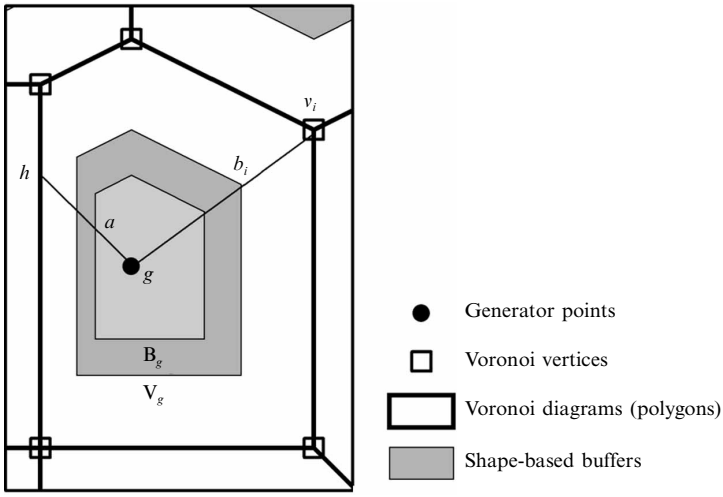

Figure 4. Constructing a shape-based point buffer.

n vertices. b_i is the vertex point of B_g corresponding to v_i. Let λ be the buffer percentage of the shape-based buffer B_g, that is, the ratio of buffer distance between this particular shape-based buffer B_g (dark gray shaded area in figure 4) and V_g, and $\lambda \in [0, 100]$.

Let x_{point}, y_{point} be the (x, y) coordinates of a point, and $\overline{gb_i}$ and $\overline{gv_i}$ the lengths of the line segments whose end points are g and b_i and g and v_i, respectively. For a given buffer percentage $\lambda = \overline{gb_i}/\overline{gv_i}$, the coordinates of vertex b_i of the shape-based buffer polygon B_g are

$$x_{b_i} = x_g + \lambda(x_{v_i} - x_g), \quad \text{and} \quad y_{b_i} = y_g + \lambda(y_{v_i} - y_g) = 1, 2, \ldots, n. \tag{2}$$

The shape-based buffer B_g can be constructed by connecting b_1 to b_2 to $\ldots$ b_n. The general construction procedure is summarized below.

1. Determine the shape of the buffers (in this example, construct the ordinary planar Voronoi diagram) for a set of known points.
2. For a given buffer percentage λ, calculate a set of buffered vertices for each generator point g using equation (2).
3. Build a shape-based buffer polygon B_g from the buffered vertices.
4. Repeat the previous two steps if multiple-ring buffers are desired.

Taking the opposite perspective, any given location a within a Voronoi polygon can be calculated to lie within λ-percent of the shape-based buffer (figure 4). Connect points g and a, extrapolate the line segment to the boundary of the closest Voronoi polygon giving intersection point h.

$$\lambda = \frac{x_a - x_g}{x_h - x_g}, \quad \lambda = \frac{y_a - y_g}{y_h - y_g}, \quad \text{and} \quad \lambda = \frac{\overline{ga}}{\overline{gh}}. \tag{3}$$

By derivation, the area ratio of the shape-based buffer B_g to the Voronoi polygon V_g can be calculated from their ratio of buffer distance λ. Let A be the area value of a polygon.

$$\frac{A_{B_g}}{A_{V_g}} = \lambda^2. \tag{4}$$

Implementation of shape-based buffers

A Visual Basic for Applications (VBA) program is developed within ArcMap™ to implement automatically the shape-based buffering process. The interface of the

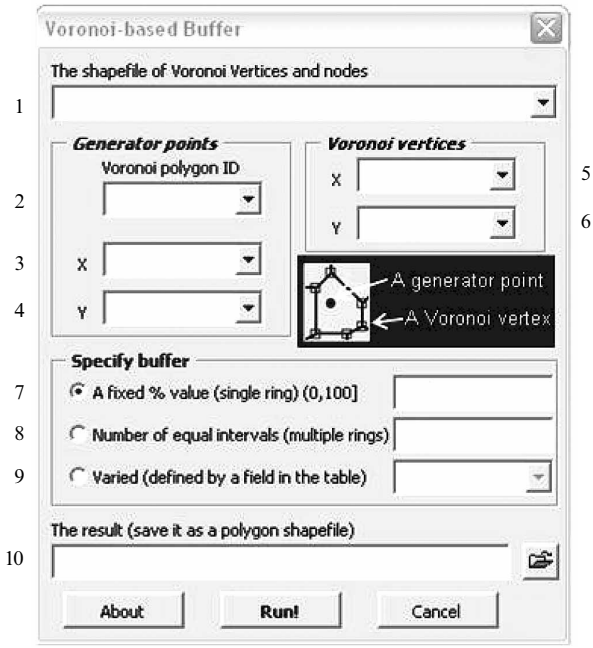

Figure 5. The interface of the shape-based buffering process in VBA (Visual Basic for Applications) program in ArcMap™.

program is shown in figure 5. The interface is designed using Voronoi polygons as the shapes, but the utility of the program is not limited to Voronoi diagrams; it can be applied to any convex shape, as discussed below. The prerequisite of the program is the input of a preprocessed, ungenerated point shapefile, which contains information such as the Voronoi generator's ID to which each Voronoi vertex belongs, the (x, y) coordinates of that Voronoi generator, and the (x, y) coordinates of the Voronoi vertices. This prerequisite can be attained through GIS topological operations. The features and functions of the VBA program are summarized in figure 5, and include the following options. (Numbers in brackets refer to the boxes in figure 5.)

- Input options: input a point shapefile with all the prerequisite information (1); specify the variable field of Voronoi generators' IDs (2); specify the variable field of the (x, y) coordinates of Voronoi generators (3 and 4); and specify the variable field of the (x, y) coordinates of Voronoi vertices (5 and 6).
- Buffering options: choose the buffering option to create a single-ring shape-based buffer, and specify the ratio of buffer distance between 0% and 100% (7); choose the buffering option to create multiple-ring shape-based buffers and specify the number of rings (8); or choose the buffering option to create a single-ring shape-based buffer, but with varied buffering ratios for each generator point, as specified in a variable field (9).
- Output options: output the buffering result as a polygon shapefile (10).

Potential applications and limitations

The shape-based buffering method has the potential to address fairness issues in arbitrary zoning. When delivering social services and emergency responses, it is desirable to balance under-served and overserved areas to achieve a degree of fairness in terms of geographic shapes. Shapes similar to those of administrative boundaries are easier to explain and more convincing than simple circles. The shape-based buffering

method can, therefore, be useful in delineating managerial or administrative boundaries in emergency preparedness and planning, and in other circumstances.

Emergency preparedness and planning

To demonstrate potential applications using the shape-based buffering method, we apply the method to three post-earthquake emergency-response-design scenarios—constructing a fixed-percentage shape-based buffer, constructing a variable-percentage shape-based buffer, and interpolating a continuous probability surface on the basis of shape-based buffering. Earthquakes are one of the most threatening natural disasters in California. The state has had an average of one seismic hazard event of magnitude 6 or higher on the Richter Scale every two to three years (Petersen et al, 1996). If the airports are undamaged and functional following an earthquake, they can play a critical role in earthquake response and recovery efforts.

The study area is the Central Coastal Region of California's Alquist–Priolo earthquake fault zones (APEFZ). The APEFZ was established by the California Geological Survey as required by the Alquist–Priolo earthquake fault zoning act, passed in 1972. The main purpose of the state law is to mitigate the hazard of surface faulting to structures for human occupancy and to prevent the construction of buildings used for human occupancy on the surface trace of active faults. Thirty-six Californian counties and one hundred cities are affected by APEFZ. These counties and cities are grouped into three geographic regions—Northern and Eastern Region, Central Coastal Region, and Southern Region (The California Geological Survey, 2006). The Central Coastal Region includes nineteen counties (figure 6). In our design scenario, all existing airports in the Central Coastal Region of the APEFZ, including international airports, general aviation airports, military airports, and federal airports will participate in the post-earthquake response. According to the *National Atlas of the United States*, there are fourteen airports in the Central Coastal Region of the APEFZ. The airports will be ensured (by means which are beyond the scope of this paper) the most expeditious return to an operational status whereby they can be used for the dispatch and delivery of emergency personnel and materials.

I demonstrate three potential applications of the shape-based buffering method—delineating an equal number of task areas while preserving the shape of a region,

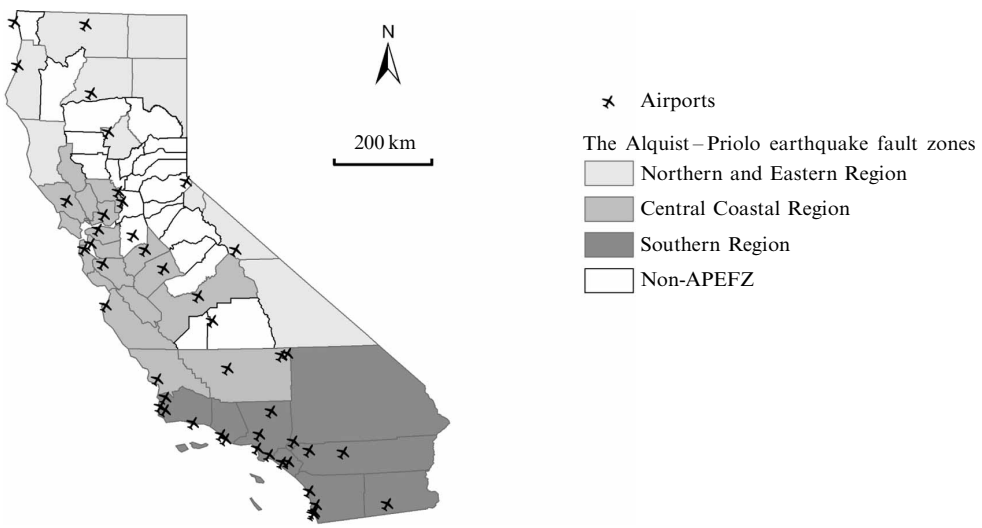

Figure 6. Airports in the Alquist–Priolo earthquake fault zones (APEFZ) in California (data sources: National Atlas of the United States and California Geological Survey).

outlining a proportional subarea within a region, and calculating the task schedule of a shape-based buffer, given a specified areal ratio. The first emergency-response task is to conduct a thorough post-earthquake survey across the whole region to evaluate damage and to determine what type of aid response is needed. Assume this task requires an airplane from each airport to fly four times within its assigned area. Each flying task occurs within a buffer ring in relation to the airport. To satisfy closeness criteria, a Voronoi diagram is constructed a priori based on the locations of the airports, and then clipped by the boundary of the study area. The clipped Voronoi polygons will serve as the coverage region for each airport. When designing a flying route, an isotropic fixed-distance approach [figure 7(a)] cannot guarantee coverage of each airport's assigned region with the same number of flying tasks. The conformal shape-based buffering [figure 7(b)], however, can fulfill the task of the delineation of equal-number task areas, while preserving the shape of a region.

The second application demonstrates that the percentage of shape-based buffers can vary from region (or point) to region (or point). Assume that within the Central Coastal Region of the APEFZ, the San Francisco Bay Area (nine counties) has a different requirement—during the same post-earthquake time frame, the survey of the Bay Area, because of its high population density and relatively compact geographic profile, requires two flying tasks, while the rest of the Central Coastal Region of the APEFZ requires four flying tasks. Thus, for the first flying task, the percentage (λ) of the shape-based buffer in the San Francisco Bay Area is 50%, but it is 25% in the rest of the region. There are six airports in the San Francisco Bay Area and eight in the rest of the Central Coastal Region of the APEFZ. Figure 8 shows the design of the first flying task. The light gray shaded area shows the San Francisco Bay Area, and the

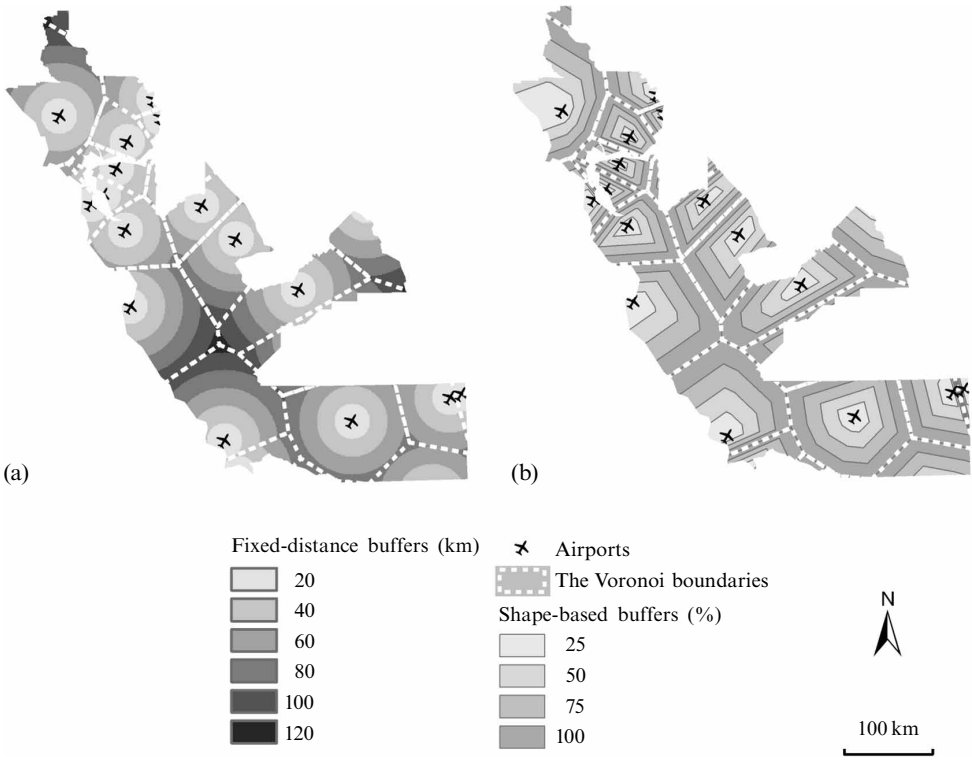

Figure 7. Constructing (a) isotropic fixed distance buffers and (b) shape-based buffers for the Central Coastal Region of the Alquist–Priolo earthquake fault zones in California.

dark gray shows the variable-percentage shape-based buffers for airports at other geographic locations. The shape-based buffering fulfills the requirements of the post-earthquake survey to outline a varied proportion of a subarea with its shape preserved.

Our third application is a continuous surface interpolation of the percentage of shape-based buffers. This can be viewed as a very finely tuned example of the first application. The generation of the surface is a routine GIS operation. The description is omitted here, but the result can provide very helpful information (figure 9). It is assumed that the need to determine when the flying survey for a given location, m, will be completed. Given the continuous surface, and equation (2), the percentage of the shape-based buffer at location m is Percentage(m) = u, $u \in [0, 100]$. If the plan for the entire area is to fly a total of n times, then location m will be surveyed at the tth time, and

$$t = \text{Round}\left(\frac{un}{100} + 0.5\right), \tag{5}$$

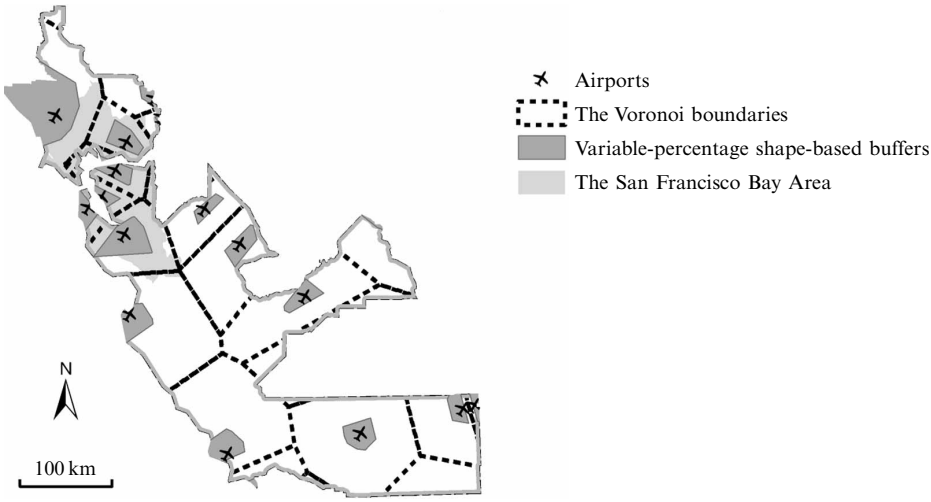

Figure 8. Shape-based buffers with variable-percentage for the Central Coastal Region of the Alquist – Priolo earthquake fault zones. San Francisco Bay Area 50%; others 25%.

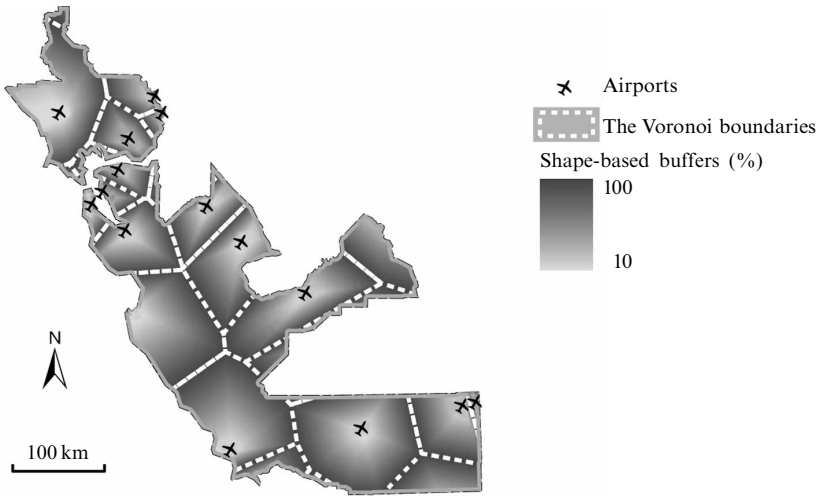

Figure 9. Constructing a shape-based buffering percentage surface.

where 'Round' is a function taking the rounded integer part of a real number. This application shows the use of the shape-based buffering percentage surface to calculate a task schedule from an opposite point of view.

Limitations and improvement

We use Voronoi diagrams to demonstrate the shape-based buffering method. The method can be extended to many shapes other than Voronoi polygons. However, the method works well only on convex shapes and some concave shapes, not on concave shapes with the generator point at a very off-center location. Using a pentagram as an example, figure 10 shows a comparison between a distance-based inner buffer and a shape-based inner buffer. The distance-based inner buffer shrinks the shape of a known polygon by offsetting a fixed distance from the boundary. For each point on the boundary, the direction of offsetting is perpendicular to it. Hence, the buffered shapes may change at certain distances due to topological merging and snapping, as shown in figure 10(a). Depending on the shape of a polygon, distance-based buffers may or may not shrink (converge) eventually to a point. In shape-based buffering, a boundary point and its corresponding buffered point are two equal-angle vectors in a polar coordinate system originating from the generator point inside the polygon, as shown in figure 4 and equation (2). Although shape-based buffering can preserve the shape of the original polygon, it cannot hold the extent of the polygon when the shape is concave, especially when the origin is not at the center of the polygon. In figure 10(b), the top diagram shows that when the origin is at, or near to, the center of the pentagram, the shapes and extents are preserved during the shape-based buffering process. However, with the origin at an off-centered location, such as in the bottom example in figure 10(b), the concave shape-based buffers may go beyond the extent of the initial polygon.

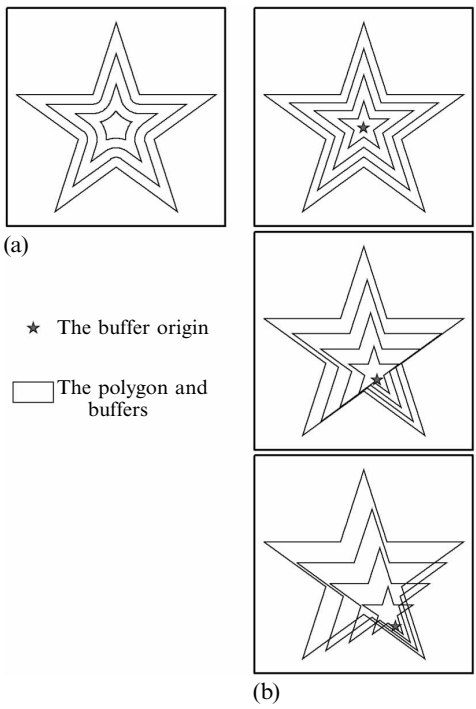

Figure 10. Limitations of shape-based buffers for concave shapes. (a) Distance-based inner buffers; (b) shape-based inner buffers.

Conclusion

Buffering is often done by incrementing the distance at constant rates in specified directions. The buffering process does not change even if the shape of spatial extent changes, and the final spatial delineation may be reached nonsimultaneously. We construct shape-based buffers from generator points and their constrained convex polygons to address the conceptual question of simultaneity in distance-based buffering. The process is conformal to the initial constraint shapes, which are predetermined by other factors or processes. This method can be applied to situations where the final scenario is preset, and the delineation of a space must be reached simultaneously. This method has potential application in emergency preparedness and response to better address fairness issues when a geographic region must be zoned arbitrarily. The limitation of the method is that when the preset shape is concave and the generator point is very off-centered, the buffered shape may not be bounded by the initial spatial extent. The method is developed and implemented using VBA scripts, and could serve the GIScience community at large.

References

Benoit D, Clark G P, 1997, "Assessing GIS for retail location planning" *Journal of Retailing and Consumer Services* **4** 239 – 258

Bolstad P, 2005 *GIS Fundamentals: A First Text on Geographic Information Systems* (Eider Press, White Bear Lake, MN)

Chakraborty J, Armstrong M P, 2001, "Assessing the impact of airborne toxic releases on populations with special needs" *The Professional Geographer* **53** 119 – 131

Chakraborty J, Schweitzer L A, Forkenbrock D J, 1999, "Using GIS to assess the environmental justice consequences of transportation system changes" *Transactions in GIS* **3** 239 – 258

Chen K, McAneney J, Blong R, Leigh R, Hunter L, Magill C, 2004, "Defining area at risk and its effect in catastrophe loss estimation: a dasymetric mapping approach" *Applied Geography* **24** 97 – 117

Cova T J, Dennison P E, Kim T H, Moritz M A, 2005, "Setting wildfire evacuation trigger points using fire spread modeling and GIS" *Transactions in GIS* **9** 603 – 617

Cringoli G, Taddei R, Rinaldi L, Veneziano V, Musella V, Cascone C, Sibilio G, Malone J B, 2004, "Use of remote sensing and geographical information systems to identify environmental features that influence the distribution of paramphistomosis in sheep from the southern Italian Apennines" *Veterinary Parasitology* **122** 15 – 26

De Genst W, Canters F, Gulinck H, 2001, "Uncertainty modeling in buffer operations applied to connectivity analysis" *Transactions in GIS* **5** 305 – 326

De Jong T, Ritsema van Eck J R, 1996, "Location profile-based measures as an improvement on accessibility modelling in GIS" *Computers, Environment and Urban Systems* **20** 181 – 190

Gething P W, Noor A M, Zurovac D, Atkinson P M, Hay S I, Nixon M S, Snow R W, 2004, "Empirical modelling of government health service use by children with fevers in Kenya" *Acta Tropica* **91** 227 – 237

Gordon-Larsen P, Nelson M C, Page P, Popkin B M, 2006, "Inequality in the built environment underlies key health disparities in physical activity and obesity" *Pediatrics* **117** 417 – 424

Hochadel M, Heinrich J, Gehring U, Morgenstern V, Kuhlbusch T, Link E, Wichmann H E, Kramer U, 2006, "Predicting long-term average concentrations of traffic-related air pollutants using GIS-based information" *Atmospheric Environment* **40** 542 – 553

Hughes M L, McDowell P F, Marcus W A, 2006, "Accuracy assessment of georectified aerial photographs: implications for measuring lateral channel movement in a GIS" *Geomorphology* **74** 1 – 16

Kramar D, Wing M G, Kennedy L, Carstensen L, Kaur T, 2005, "Relating land cover characteristics and common loon mercury levels using geographic information systems" *Ecotoxicology* **14** 253 – 262

Löfvenhaft K, Runborg S, Sjögren-Gulve P, 2004, "Biotope patterns and amphibian distribution as assessment tools in urban landscape planning" *Landscape and Urban Planning* **68** 403 – 427

Maantay J, 2007, "Asthma and air pollution in the Bronx: methodological and data considerations in using GIS for environmental justice and health research" *Health and Place* **13** 32 – 56

Mas J F, 2005, "Assessing protected area effectiveness using surrounding (buffer) areas environmentally similar to the target area" *Environmental Monitoring and Assessment* **105** 69 – 80

Narumalani S, Zhou Y, Jensen J R, 1997, "Applications of remote sensing and geographic information systems to the delineation and analysis of riparian buffer zones" *Aquatic Botany* **58** 393 – 409

Okabe A, Boots B, Sugihara K, Chiu S N, 2000 *Spatial Tessellations, Concepts and Applications of Voronoi Diagrams* (John Wiley, Chichester, Sussex)

Okamoto K, Okunuki K, Takai T, 2004, "Sketch map analysis using GIS buffer operation", in *Spatial Cognition IV, Reasoning, Action, Interaction* (Springer, Berlin) pp 227 – 244

Pereira G M, 2004, "Alternative buffer information" *GIS Science 2004* pp 239 – 250

Petersen M D, Bryant W A, Cramer C H, Cao T, Reichle M, Frankel A D, Lienkaemper J J, McCrory P A, Schwartz D P, 1996, "Probabilistic seismic hazard assessment for the State of California, California Department of Conservation, Division of Mines and Geology, Open-File Report 96 – 08", California Department of Conservation: Division of Mines and Geology, 801 K Street, MS 14-33, Sacramento, CA 95814

Pocock M J O, White P C L, McClean C J, Searle J B, 2003, "The use of accessibility in defining sub-groups of small mammals from point sampled data" *Computers, Environment and Urban Systems* **27** 71 – 83

Radke J, 1995, "Modeling urban/wildland interface fire hazards within a geographic information system" *Geographic Information Sciences* **1** 7 – 20

Radke J, Cova T, Sheridan M F, Troy A, Mu L, Johnson R, 2000, "Application challenges for GIScience: implications for research education, and policy for risk assessment, emergency preparedness and response" *The Journal of the Urban and Regional Information Systems Association* **12** 15 – 30

Ringrose S, Vanderpost C, Matheson W, 1996, "The use of integrated remotely sensed and GIS data to determine causes of vegetation cover change in southern Botswana" *Applied Geography* **16** 225 – 242

Shi W, Cheung C K, Zhu C, 2003, "Modelling error propagation in vector-based buffer analysis" *International Journal of Geographical Information Science* **17** 251 – 271

Sliva L, Williams D D, 2001, "Buffer zone versus whole catchment approaches to studying land use impact on river water quality" *Water Research* **35** 3462 – 3472

The California Geological Survey, 2006, "Alquist-Priolo Earthquake Fault Zones", http://www.consrv.ca.gov/CGS/rghm/ap/

Upchurch C, Kuby M, Zoldak M, Barranda A, 2004, "Using GIS to generate mutually exclusive service areas linking travel on and off a network" *Journal of Transport Geography* **12** 23 – 33

Vine M F, Degnan D, Hanchette C, 1998, "Geographic information systems: their use in environmental epidemiological research" *Journal of Environmental Health* **61** 7 – 16

Walker R T, Solecki W D, 1999, "Managing land use and land-cover change: the New Jersey Pinelands Biosphere Reserve" *Annals of the Association of American Geographers* **89** 220 – 237

Xiang W N, 1993, "A GIS method for riparian water-quality buffer generation" *International Journal of Geographical Information Systems* **7** 57 – 70

Xiang W N, 1996, "GIS-based riparian buffer analysis: injecting geographic information into landscape planning" *Landscape and Urban Planning* **34** 1 – 10

Xiang W N, 1998, "Assessment of the buffer-induced setback effects on riparian scenic quality by digital tools" *Environment and Planning B: Planning and Design* **25** 881 – 894

Xiang W N, Stratton W L, 1996, "The B-function and variable stream buffer mapping: a note on 'a GIS method for riparian water quality buffer generation' " *International Journal of Geographical Information Systems* **10** 499 – 510

Yin Z-Y, Walcott S, Kaplan B, Cao J, Lin W, Chen M, Liu D, Ning Y, 2005, "An analysis of the relationship between spatial patterns of water quality and urban development in Shanghai, China" *Computers, Environment and Urban Systems* **29** 197 – 221

Yu K, 1996, "Security patterns and surface model in landscape ecological planning" *Landscape and Urban Planning* **36** 1 – 17